Heavy-ion interaction in a nonisothermal plasma with two-ion correlation effects

J. D'Avanzo,[1,*] M. Lontano,[2] E. Tome',[2] and P. F. Bortignon[3]
[1]Heavy Ion Plasma Physics Group, GSI-Darmstadt, Darmstadt, Germany
[2]Istituto di Fisica del Plasma, Consiglio Nazionale delle Ricerche, EURATOM-ENEA-CNR Association, via Bassini 15, 20133 Milano, Italy
[3]Dipartimento di Fisica, Universitá di Milano, Milano, Italy
(Received 25 October 1994)

The results of a theoretical investigation of the slowing down of a heavy-ion pair, injected into a classical dense plasma with a velocity smaller than the average electron speed, are presented, paying particular attention to the two-ion correlation effects. Within the dielectric approach, both the electron and ion populations, possibly with different temperatures, are considered to participate in the plasma response via the excitation and damping of ion-acoustic and ion plasma oscillations. The electrostatic potential perturbation generated by test ion pairs and their stopping power are computed.

PACS number(s): 52.40.Mj, 28.50.$-$k

I. INTRODUCTION

The relevance to the proposed scheme of inertial confinement fusion (ICF), based on the use of heavy-ion beams (HIBs) to drive the D-T target towards the ignition conditions [1], has produced in the last few years a continuously increasing interest in the basic interaction processes occurring between ensembles of fast HIs and dense plasmas.

Several reasons support the fact that even a single HI manifests a larger stopping power in a plasma than in a cold gas due either to the higher ionization state which is established in a plasma [2] or to its more effective interaction with free electrons than with bound electrons [3].

Furthermore, it has been demonstrated that when two fast HIs, of charge states Z_1 and Z_2, move in a plasma, their behavior can be appreciably different from the predictions of single particle theories if their mutual distance d is of the order of or smaller than the effective screening length, $\lambda_{\text{eff}} \approx v_p/\omega_{pe}$ [4,5]. We note that for fast charged particles λ_{eff} is larger than the corresponding static screening length, i.e., the Debye length $\lambda_{De} = v_{\text{the}}/\omega_{pe}$ [6]. Here v_p and v_{the} are the velocity of the projectile HI and the electron thermal speed, respectively, and ω_{pe} is the electron plasma frequency. This "modified" interaction can be easily explained by assuming that when $d \ll \lambda_{\text{eff}}$ the plasma response to two test ions is that it would manifest in the presence of a single projectile having a total charge almost equal to Z_1+Z_2. Since the stopping power of a charged particle is proportional to Z^2, the important role of "vicinity" effects (which we shall call "two-ion correlation" effects) is evident.

Two-ion correlation effects on the stopping power of a couple of HIs, traveling along a straight trajectory, with the same fixed velocity $\mathbf{v}_p$, have been previously investigated in the limit of fast projectiles, i.e., $v_p \gg v_{\text{the}}$ [4,5,7], by neglecting the response of the plasma ions due to their large mass. In particular, in Ref. [4] the consequences of an average procedure over a uniform angular distribution of the interionic vector $\mathbf{d}$ have been considered; in Refs. [5,7] the influence of the closeness of two aligned (i.e., with $\mathbf{d}\times\mathbf{v}_p=0$) ions on their stopping power has been evaluated; finally, in Ref. [7] the forces acting on the two ions, and induced by their motion in a dispersive plasma, have been investigated in detail for an arbitrary orientation of the vector $\mathbf{d}$.

When most of the slowing down process of the incoming ions occurs at velocities lower than v_{the}, in general a correct evaluation of the stopping power, and then of the relevant correlation effects, requires that plasma ion dynamics is retained as well [8,9].

In the present paper a detailed analysis of the electrostatic potential induced by two "close" projectile ions traveling in a two-component (electrons and ions), nonisothermal ($T_e \neq T_i$) plasma is presented together with the evaluation of the relevant stopping power and power deposition profiles, retaining two-ion correlation effects [10].

Besides the interest of principle for the physical problem of the stopping power of mutually correlated charged particles, its relevance for the ICF is motivated by the proposed scheme which foresees the use of cluster ion beams (CIBs) [11], instead of conventional HIBs, to drive the target towards the ignition, due to their much stronger interaction with matter and to the reduced beam current during the acceleration phase. When a molecular cluster penetrates the matter (which we shall assume to be already in the state of plasma), the Coulomb explosion creates a swarm of debris, whose dynamics is strongly correlated due to their small mutual distances (of the order of a few Å). Moreover, due to their large mass, to deposit the required amount of energy into the target, a limited cluster velocity is sufficient. A detailed discussion of the potentialities of CIB in ICF can be found in Ref. [12].

In Sec. II the potential wake generated by HIs in nonisothermal plasmas and the relevant stopping power are first computed in the one-dimensional (1D) case. The full

*On leave from Dipartimento di Ingegneria Nucleare, Politecnico di Milano, Milano, Italy.

three-dimensional (3D) analysis of the interaction of HIs in nonequilibrium plasmas is then considered in Sec. III. Here, a detailed study of the electrostatic potential induced by a single slow ion and the stopping process of an uncorrelated particle and of two correlated ions in a two-temperature plasma are discussed. Section IV is devoted to the summary of the results and to their discussion. The discussion on the choice of the upper cutoff in the k integration occurring in computing the stopping power can be found in the Appendix.

II. HEAVY-ION STOPPING IN DENSE PLASMAS: 1D CASE

Let us consider first a fully ionized collisionless plasma composed of electrons and ions, of charge number Z_i. Let each species be characterized by its own unperturbed density $n_{\alpha 0}$ and temperature T_α, with $\alpha=e,i$, respectively, with $Z_i n_{i0}=n_{e0}$.

In this section we perform a preliminary analysis of the stopping properties of a dense nonisothermal plasma by assuming that the system remains uniform and unperturbed in the plane (y,z) perpendicular to the direction of motion of the projectile ions, the x axis. This corresponds to considering the stopping process of charged sheets moving along the x direction.

The plasma response to external perturbations can be described on the basis of a kinetic theory in terms of the distribution functions $f_\alpha(x,\mathbf{v},t)=\delta(v_y)\delta(v_z)F_\alpha(x,v_x,t)$, which satisfy the Vlasov equations

$$\frac{\partial F_e}{\partial t}+v\frac{\partial F_e}{\partial x}+\frac{\partial \phi}{\partial x}\frac{\partial F_e}{\partial v}=0\ , \tag{2.1a}$$

$$\frac{\partial F_i}{\partial t}+v\frac{\partial F_i}{\partial x}-\frac{1}{M}\frac{\partial \phi}{\partial x}\frac{\partial F_i}{\partial v}=0\ . \tag{2.1b}$$

Here, the following dimensionless quantities have been introduced:

$$x\to\frac{x}{\lambda_{De}}\ ,\quad v\to\frac{v_x}{v_{\mathrm{the}}}\ ,\quad t\to\omega_{pe}t\ ,$$
$$\phi\to\frac{e\phi}{T_e}\ ,\quad f_\alpha\to\frac{v_{\mathrm{th}\alpha}}{n_{\alpha 0}}f_\alpha\ , \tag{2.2}$$

and $\lambda_{De}=(T_e/4\pi n_{e0}e^2)^{1/2}$, $v_{\mathrm{th}\alpha}=(T_\alpha/m_\alpha)^{1/2}$, $\omega_{pe}=v_{\mathrm{the}}/\lambda_{De}$, $M=m_i/m_e$. For the sake of simplicity a hydrogen plasma ($Z_i=1$, $M=1840$) has been considered.

The electrostatic (ES) potential $\phi(x,t)$ represents the perturbation induced by the transit of two projectile ions (positively charged sheets) with the same charge state Z_{eff}, moving with the same velocity v_p and separated by a fixed distance d, and is consistently described by the Poisson equation

$$\frac{\partial^2\phi}{\partial x^2}=-Z\delta(x-v_pt)-Z\delta[x-(v_pt+d)]+\sum_{\alpha=e,i}\left[\frac{m_\alpha}{m_e}\right]^{1/2}\left[\frac{T_\alpha}{T_e}\right]^{1/2}\frac{n_{\alpha 0}}{n_{e0}}\times\int_{-\infty}^{+\infty}dv'F_\alpha(x,v',t)\ , \tag{2.3}$$

where $Z=(Z_{\mathrm{eff}}/n_{e0}^{(1)}\lambda_{De})(n_p^{(2)}/n_e^{(2)})$ is the interaction parameter, $n_e^{(1)}$ is the unperturbed line (along x) electron density, $n_e^{(2)}$ is the surface (in the plane y,z) electron density, and $Z_{\mathrm{eff}}n_p^{(2)}$ is the surface charge distribution of the projectile ions. These latter two quantities are assumed to be constant.

The Vlasov-Poisson system (2.1), (2.3) can be linearized when the interaction is weak, that is, for $Z\ll 1$. In this case, by using standard techniques of Laplace-Fourier transforms, it is possible to obtain the first order ES potential induced by the presence of the two ions in a nonisothermal unidimensional plasma; it reads

$$\phi_1(x,t)=\frac{Z}{2\pi}\int_{-\infty}^{+\infty}dk\frac{e^{ikx}}{k^2\varepsilon(|k|,kv_p)}(1+e^{-ikd})\ , \tag{2.4}$$

where the explicit form of the dielectric function is

$$\varepsilon(|k|,kv_p)=1+\frac{1}{k^2}\sum_{\alpha=e,i}\frac{T_e}{T_\alpha}\frac{n_\alpha}{n_e}W\left[\left[\frac{T_e}{T_\alpha}\right]^{1/2}\left[\frac{m_\alpha}{m_e}\right]^{1/2}\frac{kv_p}{|k|}\right] \tag{2.5}$$

and $W(\zeta)=X(\zeta)+i(\zeta)$ is the plasma dispersion function [6]. Here, unperturbed Maxwellian distributions have been assumed.

Before going into the discussion of the stopping power of the injected ions, we spend a few words on the ES potential distribution $\phi_1^{(1)}(x,t)$ induced by a single ion moving with a given velocity v_p. Due to the linear character of our analysis, it will then be straightforward to find the potential created by the ion pair. Let us notice that the ion thermal velocity $v_{\mathrm{th}i}=\sqrt{T_i/m_i}$ and the ion-acoustic speed $c_s=\sqrt{T_e/m_i}$ in dimensionless units read $v_{\mathrm{th}i}=T^{-1/2}M^{-1/2}$ and $c_s=M^{-1/2}$, respectively. In Fig. 1 we have plotted the potential $\phi_1^{(1)}$ as a function of the coordinate $x-v_pt\to\xi$ due to a charge $Z=1$ placed at $\xi=0$, for different values of the ion velocity, i.e., $v_p=0.001$ (a), 0.0136 (b), 0.0184 (c), 0.022 (d), 0.5 (e). The value $T\equiv T_e/T_i=36$ has been chosen. It is seen that by increasing the particle velocity from $v_p<T^{-1/2}M^{-1/2}$ (a) to $M^{-1/2}<v_p<1$ (e), corresponding to two situations in which the particle is dynamically screened, respectively, by the ions or by the electrons, physical conditions can be found which are characterized by the excitation of both strongly damped [(b) and (d)] and weakly damped (c) plasma oscillations. These last plots refer to $T^{-1/2}M^{-1/2}<v_p<M^{-1/2}$, an interval existing only in nonisothermal plasmas, i.e., for $T>1$. By expanding the plasma dispersion function relevant to the electrons for small argument and that of the ions for large argument, Eq. (2.5) can be computed analytically and the potential takes the form

$$\phi_1^{(1)} = \frac{Z v_p}{\beta} \Theta(-\xi) \sin\left[\frac{\xi}{v_p}\beta\right], \tag{2.6}$$

where $\beta^2 = M^{-1} - v_p^2 > 0$. Equation (2.6) describes the undamped induced oscillation, that is, it does not contain the effect of Landau damping.

This preliminary study of the characteristics of the potential perturbation induced in a nonequilibrium plasma by a test ion, and the appearance of velocity intervals in which the excitation of long-range plasma oscillations occurs, supports the further search for the two-ion correlation effects on the stopping power when the average interionic distance d is comparable to or smaller than the typical wavelength of the excited oscillations.

Let us introduce the stopping power for a couple of ions traveling in a plasma composed by electrons and a thermal ion species. It reads

$$-\frac{dE}{dx} = \mathbf{F}\cdot\hat{\mathbf{e}}_x|_{\xi=0} + \mathbf{F}\cdot\hat{\mathbf{e}}_x|_{\xi=-v_p\tau}$$
$$= ZN_D \left\{ \left.\frac{\partial\phi_1}{\partial\xi}\right|_{\xi=0} + \left.\frac{\partial\phi_1}{\partial\xi}\right|_{\xi=-v_p\tau} \right\}, \tag{2.7}$$

where $N_D = n_{e0}\lambda_{De}^3 \gg 1$. Again, by suitable expansions of the plasma dispersion function, we can approximate the stopping power of a single ion, depending on its velocity, by the equation

$$-\frac{dE}{dx} \approx \frac{1}{2} Z^2 N_D \gamma , \tag{2.8}$$

where

$$\gamma = 1 \quad \text{for } v_p > 1 \text{ and } (MT)^{-1/2} < v_p < M^{-1/2} ,$$

$$\gamma = \frac{1}{\sqrt{2\pi}} \frac{v_p}{1 - 1/M v_p^2} \quad \text{for } M^{-1/2} < v_p < 1 ,$$

$$\gamma = \frac{v_p}{\sqrt{2\pi}} \frac{1 + T^{3/2} M^{1/2}}{1 + T} \quad \text{for } 0 < v_p < (MT)^{-1/2} .$$

As an example, in Fig. 2 the stopping power (normalized to $Z^2 N_D/2$) of a single ion is plotted for $v_p < 1$, and different temperature ratios, $T = 2.25, 9, 49$. For $T = 49$, the ion thermal speed $v_p = (MT)^{-1/2} = 0.003$ and the ion-acoustic velocity $v_p = M^{-1/2} = 0.023$, and in this interval a strong enhancement of the stopping power occurs for $T \gg 1$.

Coming now to the slowing down process of an ion pair, Fig. 3 shows the stopping power (normalized to $Z^2 N_D/2$) versus v_p for two equally charged ions, $d = 30$ away from each other, for $T = 25$ and 100. It can be not-

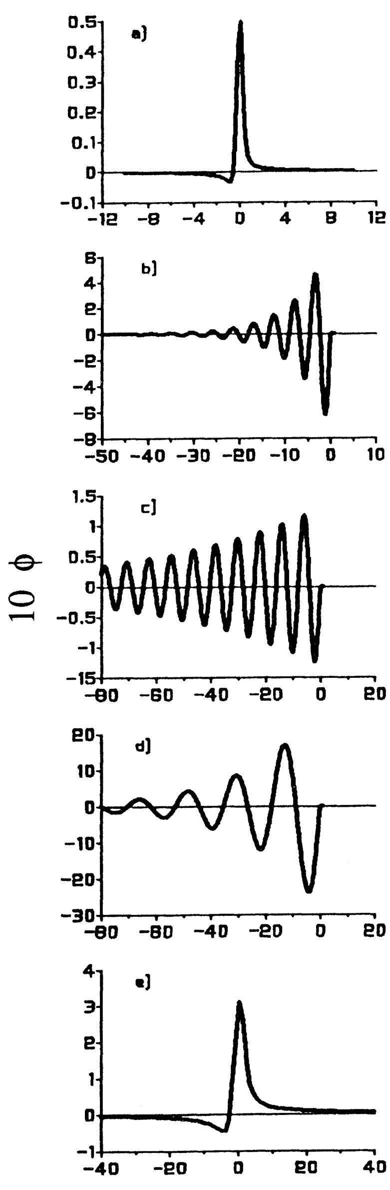

FIG. 1. One-dimensional ES potential $\phi_1^{(1)}$ (in units of T_e/e), induced by the presence of a moving charged particle, with $Z = 1$, in a nonisothermal plasma, as a function of the spatial coordinate $\xi = x - v_p t$ (in units of λ_{De}), for $T = 36$ and $v_p = 0.001$ (a), 0.0136 (b) 0.0184 (c), 0.022 (d), and 0.5 (e). Here $v_{\text{th}i} \approx 0.004$ and $c_s \approx 0.023$. All the quantities are normalized according to Eqs. (2.2).

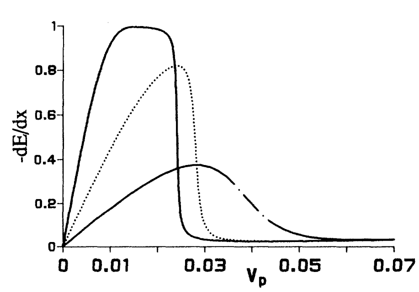

FIG. 2. The stopping power $-dE/dx$ [in units of $(Z^2 N_D/2)(T_e/e)$] of a single ion moving in a nonisothermal plasma is plotted versus v_p (in units of v_{th_e}) for $v_p < 1$. Here, $T = 2.25$ (dash-dotted line), 9 (dotted line), and 49 (continuous line).

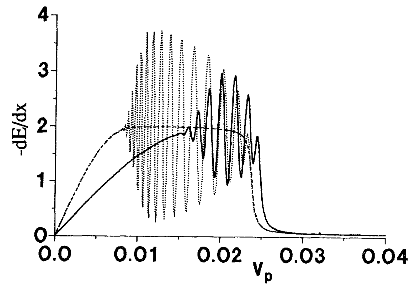

FIG. 3. The stopping power $-dE/dx$ [in units of $(Z^2N_D/2)(T_e/e)$] of a system of two equally charged ions, separated by a distance $d/\lambda_{De}=30$, is plotted versus v_p (in units of v_{the}), for $T=25$ (continuous line) and 100 (dotted line). Dashed line refers to the system of two uncorrelated ions (corresponding to $d=\infty$).

ed that by increasing the nonisothermicity of the plasma (with $T\gg1$), the range of projectile velocities affected by correlations increases as well.

When an ion pair is moving in a one-dimensional plasma, the stopping power of the whole system turns out to be modified with respect to that predicted by an uncorrelated particle model. By introducing the expansions of the plasma dispersion function, it is possible to derive approximate analytical expressions for the stopping power of the two-ion system. We have

$$-\frac{dE}{dx}\cong\left[\frac{2}{\pi}\right]^{1/2}\frac{Z^2N_Dv_p}{\eta^2}\times\left\{1+\frac{1}{8}\eta v_p\tau[e^{-\eta v_p\tau}(\mathrm{Ei}(\eta v_p\tau)-E_1(\eta v_p\tau))+2e^{\eta v_p\tau}E_1(\eta v_p\tau)]\right\}, \quad (2.9)$$

with $\eta=\sqrt{1-1/Mv_p^2}$, for $M^{-1/2}\ll v_p\ll1$, and

$$-\frac{dE}{dx}\cong Z^2N_D[1+\cos(\eta' v_p\tau)], \quad (2.10)$$

with $\eta'=\sqrt{1/Mv_p^2-1}$, for $(MT)^{-1/2}\ll v_p\ll M^{-1/2}$.

Ei and E_1 are the exponential integral functions [13].

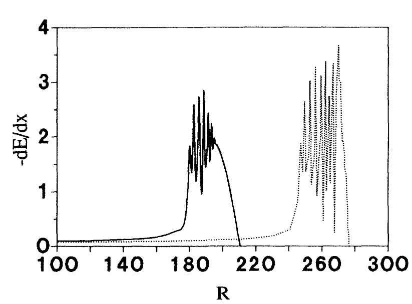

FIG. 4. Energy deposition profile, $-dE/dx$ (in units of T_e/λ_{De}), versus $R(v)$ (in units of λ_{De}), for an ion pair with $v_p=0.03$ and $m_p=40$ amu. Other parameters are the same as in Fig. 3.

The power deposition profile of a charged particle can be obtained from the knowledge of the *partial range,* that is, of the function $R(v)$,

$$R(E)=-\int_{E_{\mathrm{in}}}^{E}dE'\left[-\frac{dE'}{dx}\right]^{-1}, \quad (2.11)$$

where in dimensional units $E=m_pv^2/2$. In Fig. 4 the normalized stopping power (function of v) of two correlated ions is shown versus $R(v)$, for the same parameters as in Fig. 3. The injection velocity of the two particles is $v_p=0.03$ and $m_p=40$ amu.

III. HEAVY-ION STOPPING IN DENSE PLASMAS: 3D CASE

In this section, we extend the analysis of the stopping properties of a nonisothermal plasma to the three-dimensional case. Again, the two-component background plasma is assumed to be Maxwellian with $T_e\neq T_i$. The relevant dimensionless linearized equations for the first order distribution function of the α species, $f_{1\alpha}(\mathbf{r},\mathbf{v},t)$, and for the associated ES potential perturbation, $\phi_1(\mathbf{r},t)$, are now

$$\frac{\partial f_{1e}}{\partial t}+\mathbf{v}\cdot\frac{\partial f_{1e}}{\partial\mathbf{r}}+\frac{\partial\phi_1}{\partial\mathbf{r}}\cdot\frac{\partial f_{0e}}{\partial\mathbf{v}}=0, \quad (3.1a)$$

$$\frac{\partial f_{1i}}{\partial t}+\mathbf{v}\cdot\frac{\partial f_{1i}}{\partial\mathbf{r}}-\frac{1}{M}\frac{\partial\phi_1}{\partial\mathbf{r}}\cdot\frac{\partial f_{0i}}{\partial\mathbf{v}}=0, \quad (3.1b)$$

$$\nabla^2\phi_1=-Z\delta(\mathbf{r}-\mathbf{v}_pt)-Z\delta[\mathbf{r}-(\mathbf{v}_pt+\mathbf{d})]+\int d^3v\,f_{1e}(\mathbf{r},\mathbf{v},t)-(TM)^{3/2}\int d^3v\,f_{1i}(\mathbf{r},\mathbf{v},t), \quad (3.1c)$$

where the dimensionless variables

$$\mathbf{r}\to\frac{\mathbf{r}}{\lambda_{De}},\quad \mathbf{v}\to\frac{\mathbf{v}}{v_{\mathrm{the}}},\quad t\to t\omega_{pe},\quad \phi\to\frac{e\phi}{T_e},\quad f_\alpha\to f_\alpha\frac{v_{\mathrm{th}\alpha}^3}{n_\alpha}\quad(\alpha=e,i) \quad (3.2)$$

have been introduced. Again, $T=T_e/T_i$, $M=m_i/m_e$, $v_{\mathrm{th}\alpha}=(T_\alpha/m_\alpha)^{1/2}$, $\lambda_{De}=(T_e/4\pi ne^2)^{1/2}$, $\omega_{pe}=v_{\mathrm{the}}/\lambda_{De}$. A hydrogen background plasma is considered.

Equation (3.1c) contains two pointlike HIs as source terms, placed at $\mathbf{r}=\mathbf{v}_pt$ and $\mathbf{r}=\mathbf{v}_pt+\mathbf{d}$, where $\mathbf{v}_p$ and $\mathbf{d}$ are assumed to be given constant vectors. Later on, when two-ion correlations will be discussed, the particular case of aligned ions (i.e., $\mathbf{d}\|\mathbf{v}_p$) will be considered.

A. The electrostatic potential induced by a single test ion

By Fourier-Laplace transforming Eqs. (3.1), we obtain the asymptotic form of the linearized ES potential $\phi_1(\mathbf{r},t)$ generated in the plasma by the two ions:

$$\phi_1(\mathbf{r},t)=\frac{Z}{(2\pi)^3}\int d^3k\frac{e^{i\mathbf{k}\cdot(\mathbf{r}-\mathbf{v}_pt)}}{k^2\varepsilon(\mathbf{k},\mathbf{k}\cdot\mathbf{v}_p)}(1+e^{-i\mathbf{k}\cdot\mathbf{d}}), \quad (3.3)$$

where the dielectric function for longitudinal oscillations is

$$\varepsilon(\mathbf{k},\omega)=1+\frac{1}{k^2}\left[W\left[\frac{\omega}{k}\right]+TW\left[T^{1/2}M^{1/2}\frac{\omega}{k}\right]\right] . \quad (3.4)$$

In the linear approximation, the potential distribution created by the two ions is the superposition of the distributions associated with each of the two projectiles. Let us consider, for simplicity, the potential created by a single ion, and introduce the reference frame moving with the velocity $\mathbf{v}_p$, and such that the source charge is placed at its origin. With the ξ axis along $\mathbf{v}_p$, we can introduce the position vector $\mathbf{r}=\xi\hat{\mathbf{e}}_x+\rho\hat{\mathbf{e}}_\rho$. The ES potential then takes the form

$$\phi_1^{(1)}(\mathbf{r})=\frac{Z}{4\pi^2}\int_0^\infty dk\int_{-1}^{+1}d\mu\frac{e^{ik\xi\mu}}{\varepsilon(\mathbf{k},kv_p\mu)}J_0(k\rho\sqrt{1-\mu^2}) , \quad (3.5)$$

where J_0 is the Bessel function of zero order, $\mu=\cos\theta$, and θ is the angle between $\mathbf{k}$ and $\mathbf{v}_p$.

The explicit computation of the integral in Eq. (3.5) has been performed either numerically or analytically, under *ad hoc* assumptions, in the velocity ranges $[0,v_{\text{th}i}]$, $[v_{\text{th}i},c_s]$, $[c_s,v_{\text{th}e}]$ for $T>1$. Here $c_s=(T_e/m_i)^{1/2}$ is the ion-sound speed.

1. *Electrostatic potential for* $v_p \ll v_{thi}$ $[v_p \ll (TM)^{-1/2}]$

For small projectile velocities by expanding $W(\zeta)$ for $\zeta \ll 1$, Eq. (3.5) can be approximately written as the sum of two contributions

$$\phi_1^{(1)}(\mathbf{r})=\phi^0(\mathbf{r})+\phi^1(\mathbf{r}) , \quad (3.6)$$

where

$$\phi^0(r)=\frac{Z}{4\pi}\frac{e^{-\beta r}}{r} , \quad (3.7)$$

$$\begin{aligned}\phi_1(\mathbf{r})=&\frac{Z}{4(2\pi)^{3/2}}\frac{\mathbf{v}_p\cdot\mathbf{r}}{\beta r}(1+T^{3/2}M^{1/2})\\&\times\{[1+\beta r+(\beta r)^2]e^{-\beta r}\text{Ei}(\beta r)\\&+[1-\beta r+(\beta r)^2]e^{\beta r}E_1(\beta r)-2\beta r\}+O(v_p^2) ,\end{aligned} \quad (3.8)$$

$\beta=\sqrt{1+T}$, and $r=\sqrt{\xi^2+\rho^2}$. Equations (3.7) and (3.8) represent a vacuum ES potential screened on a distance $\lambda_D=\lambda_{De}/\sqrt{1+T}$, plus a linear (in $\hat{\mathbf{e}}_r\cdot\mathbf{v}_p$) correction.

2. *Electrostatic potential for* $v_{thi} \ll v_p \ll c_s$ $[(TM)^{-1/2} \ll v_p \ll M^{-1/2}]$

When $T \gg 1$ it is possible to neglect the electron contribution in the real part of $\varepsilon(\mathbf{k},\omega)$, i.e., $k^2\varepsilon \approx k^2-(Mv_p^2\mu^2)^{-1}$. Therefore the zeros of the denominator exist only for k values belonging to the interval $[0,T^{1/2}]$. This suggests splitting the k integral in Eq. (3.5) as follows:

$$\phi_1^{(1)}(\mathbf{r})=\phi_{k<\sqrt{T}}(\mathbf{r})+\phi_{k>\sqrt{T}}(\mathbf{r}) . \quad (3.9)$$

Moreover, the condition $k>1/M^{1/2}v_p$ makes the denominator in $\phi_{k<\sqrt{T}}$ vanish for $\mu=\mu_\pm\approx\pm 1/kM^{1/2}v_p$, with $|\mu_\pm|<1$. $\phi_{k<\sqrt{T}}$ is then written as the sum of two contributions, as

$$\phi_{k<\sqrt{T}}(\mathbf{r})=\phi'(\mathbf{r})+\phi''(\mathbf{r}) , \quad (3.10)$$

where

$$\phi'(\mathbf{r})=\frac{z}{4\pi^2}\int_0^{1/\sqrt{M}v_p}dk\int_{-1}^{+1}d\mu\frac{e^{ik\xi\mu}J_0(k\rho\sqrt{1-\mu^2})}{1+\frac{1}{k^2}\left\{-\frac{1}{Mv_p^2\mu^2}+i\left[\frac{\pi}{2}\right]^{1/2}v_p\mu\left[e^{-v_p^2\mu^2/2}+T^{3/2}M^{1/2}e^{-TMv_p^2\mu^2/2}\right]\right\}} , \quad (3.11)$$

$$\phi''(\mathbf{r})=\frac{Z}{4\pi^2}\int_{1/\sqrt{M}v_p}^{\sqrt{T}}dk\oint d\mu\frac{e^{ik\xi\mu}J_0(k\rho\sqrt{1-\mu^2})}{1+\frac{1}{k^2}\left\{-\frac{1}{Mv_p^2\mu^2}+i\left[\frac{\pi}{2}\right]^{1/2}v_p\mu\left[e^{-v_p^2\mu^2/2}+T^{3/2}M^{1/2}e^{-TMv_p^2\mu^2/2}\right]\right\}} . \quad (3.12)$$

$\phi''(\mathbf{r})$ turns out to have an oscillating character to which the elementary modes with $\lambda>\lambda_{Di}$ contribute.

We report in the following the approximate expressions of the potential distributions $\phi_{k<\sqrt{T}}$ and $\phi_{k>\sqrt{T}}$ in the particular case of $\rho=0$ (except for ϕ'', whose dependences both on ξ and ρ are evidenced), that is along the ξ axis:

$$\begin{aligned}\phi'(\xi,\rho=0)\cong\frac{Z}{2\pi^2}\frac{Mv_p^2}{\xi^2}&\left[\frac{1}{\sqrt{M}v_p}\cos\left[\frac{\xi}{\sqrt{M}v_p}\right]\right.\\&-\left[1+\frac{2}{\xi}\right]\sin\left[\frac{\xi}{\sqrt{M}v_p}\right]\\&\left.+\frac{2}{\xi}\,\text{Si}\left[\frac{\xi}{\sqrt{M}v_p}\right]\right] ,\end{aligned} \quad (3.11')$$

$$\phi''(\xi,\rho)\cong\frac{\sqrt{3}Z}{2\pi}H\left[-\xi-\rho\frac{\sqrt{TM}v_p}{\sqrt{3}}\right]\frac{e^{-\Gamma|\xi|}}{\sqrt{T}Mv_p^2}\times\frac{\cos[\sqrt{3\xi^2/TM^2v_p^2-\rho^2/Mv_p^2}]}{\sqrt{3\xi^2/TM^2v_p^4-\rho^2/Mv_p^2}}\ . \quad (3.12')$$

Moreover, we have

$$\phi_{k>\sqrt{T}}(\mathbf{r})=\phi^1(\mathbf{r})+\phi^2(\mathbf{r})+\phi^3(\mathbf{r})\ , \quad (3.13)$$

with

$$\phi^1(\xi,\rho=0)\cong-\frac{Z}{2\pi^2}\frac{1}{\xi}\operatorname{si}(\sqrt{T}\,\xi)\ , \quad (3.14)$$

$$\phi^2(\xi,\rho=0)\cong-\frac{Z}{2\pi^2}\frac{1}{\sqrt{M}v_p}\int_0^{\sqrt{TM}v_p}dtX(t)\ , \quad (3.15)$$

$$\phi^3(\xi,\rho=0)\cong\frac{Z}{8\pi}\frac{\xi}{v_p^2}\left[E_1\left[\frac{T\xi^2}{2v_p^2}\right]+\frac{1}{M}E_1\left[\frac{\xi^2}{2Mv_p^2}\right]\right]\ , \quad (3.16)$$

and X is the real part of the plasma dispersion function (see Sec. II). Equation (3.12′) describes the Cherenkov cone of ion plasma and ion-sound oscillations following the test ion. Its semiaperture is $\alpha=\tan^{-1}(\sqrt{3/TMv_p^2})$ which manifests a dependence on the temperature ratio, besides that on the particle velocity. A constant approximated damping rate Γ in Eqs. (3.12′) has been introduced following the considerations by Peter [14]. The function $\operatorname{Si}(z)$ is the sine integral function and $\operatorname{si}(z)=\operatorname{Si}(z)-\pi/2$. They are defined in Ref. [13].

3. *Electrostatic potential for $c_s \ll v_p \ll v_{the}$ $[M^{-1/2} \ll v_p \ll 1]$*

The expansion of the electron and ion susceptibilities for small and large argument, respectively, allows one to evaluate the dielectric function as $k^2\varepsilon(k,k\mu v_p)\cong k^2+1-1/M\mu^2v_p^2$. For $v_p>M^{-1/2}$, the μ integration should be performed taking account of the presence of two symmetric poles at $\mu_\pm=\pm[(k^2+1)Mv_p^2]^{-1/2}$. To get an approximated semianalytical expression for the ES potential, it is possible to substitute the integral in μ, between -1 and $+1$, with an integration along a closed circuit which is obtained by closing the straight path from -1 to $+1$ with the half circle, in the upper part of the μ plane, proceeding from $+1$ to -1, following the procedure discussed by Peter in Ref. [14].

If the poles are situated sufficiently close to the real-k axis, the following approximate expression is found to be valid along the direction of the ion motion ($\rho=0$):

$$\phi_1(\xi,\rho=0)\cong\frac{Z}{2\pi\sqrt{M}v_p}H(-\xi)\int_0^\infty dk\frac{k^2}{(k^2+1)^{3/2}}\sin\left[\frac{k}{(k^2+1)^{1/2}}\frac{\xi}{\sqrt{M}v_p}\right]\times\exp\left\{-\left[\frac{\pi}{8}\right]^{1/2}\frac{k^2}{(k^2+1)^2}\frac{|\xi|}{Mv_p}[e^{-1/[2M(k^2+1)]}+T^{3/2}M^{1/2}e^{-T/[2(k^2+1)]}]\right\}\ . \quad (3.17)$$

We observe that both in the case described in Sec. III A 2 [see Eq. (3.11′)] and that described in Sec. III A 3 [see Eq. (3.17)] the ES potential excited by the transit of the test ion has oscillating contributions characterized by a typical wavelength of the order $\lambda\approx2\pi M^{1/2}v_p$, independent of the temperature ratio T.

Numerical integration of Eq. (3.15) has been performed by retaining the full expression of the dielectric function [see Eq. (3.4)]. In Fig. 5 the dimensionless ES potential ϕ_1 is plotted versus the ξ coordinate for $\rho=0$, $v_p=0.02$, $Z=0.077$ (corresponding to $Z_{\text{eff}}=10$, $T_e=100$ eV, and $n_e=10^{19}$ cm^{-3}), and for different values of T: 0.33 (curve a), 1 (curve b), 3 (curve c), 10 (curve d). Here $\lambda_{De}\approx0.02$ μm. In Fig. 6 ϕ_1 versus ξ is shown for $T=10$ ($T_e=100$ eV, $T_i=10$ eV) and different values of v_p: 0.005 (curve a), 0.01 (curve b), 0.02 (curve c), 0.04 (curve d), 0.1 (curve e). We remind the reader that the reference frame moving at $\mathbf{v}_p$ has been introduced ($x-v_pt\to\xi$). From inspection of Fig. 6 it is observed that depending on the particle velocity different regimes of wave excitation occur. For example, at low velocities [i.e., $v_p<(TM)^{-1/2}$, as for curve *a*], only a limited deformation of the static Debye screening is produced. In the range $(TM)^{-1/2}<v_p<M^{-1/2}$ (corresponding to curves *b* and *c*) oscillations with a typical

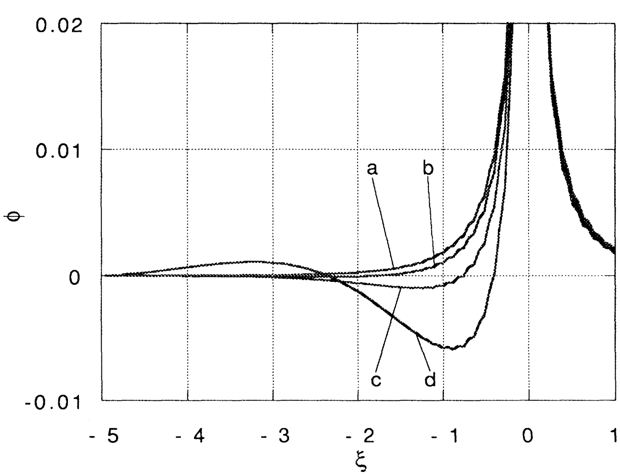

FIG. 5. Three-dimensional ES potential (in units of T_e/e), for $\rho=0$, versus $\xi=x-v_pt$ (in units of λ_{De}), induced in a nonisothermal plasma by the transit of a single charged particle with $v_p=0.02$, $Z=0.077$, and for $T=0.33$ (curve *a*), 1 (curve *b*), 3 (curve *c*), and 10 (curve *d*). All the quantities are normalized according to Eqs. (2.2). Here the corresponding dimensional parameters are $n_e=10^{19}$ cm^{-3}, $T_e=100$ eV, $Z_{\text{eff}}=10$.

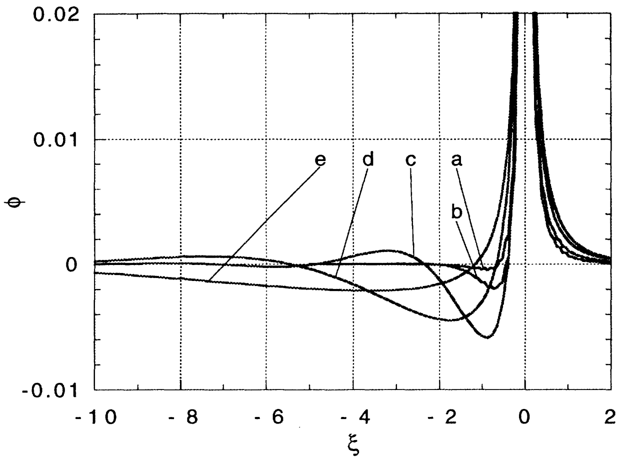

FIG. 6. Three-dimensional ES potential (normalized to T_e/e), for $\rho=0$, versus $\xi=x-v_p t$ (in units of λ_{De}), induced in a nonisothermal plasma by the transit of a single charged particle with $T=10$, $Z=0.077$, and for $v_p=0.005$ (curve a), 0.01 (curve b), 0.02 (curve c), 0.04 (curve d), and 0.1 (curve e). The corresponding dimensional parameters are the same as in Fig. 5.

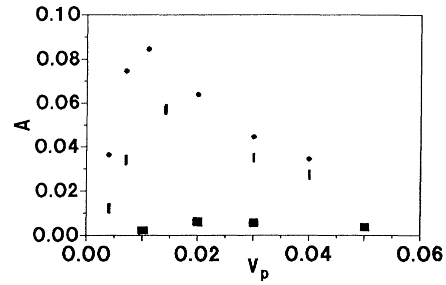

FIG. 7. The amplitude A (normalized to T_e/e) of the first ES potential well behind the charged particle, moving in a nonisothermal plasma, as a function of the particle velocity v_p (in units of v_{the}), for $T=10$ and $Z=0.077$ (■), and for $T=49$ (▮), 100 (●), and $Z=0.24$.

wavelength of the order of λ_{De} appear. At supersonic velocities, i.e., $v_p > M^{-1/2}$ (curves d and e), long wavelength oscillations are excited. We remind the reader that for the projectile-plasma parameters considered, $(TM)^{-1/2} \approx 0.0074$ and $M^{-1/2} \approx 0.023$.

By defining L as the distance between the first two zeros of the potential, and A the maximum amplitude (better, its modulus) of the potential well following the projectiles, a numerical study of the dependence of the potential perturbation on the physical parameters has been performed. In Fig. 7 the amplitude A versus the particle velocity v_p is shown for different values of T (10, 49, 100). It is shown that the normalized amplitude of the potential well increases with the temperature anisotropy, due to the corresponding increase in the efficiency of ion-acoustic wave excitation. Moreover, the curves are characterized by a maximum around the ion-sound speed. At increasing velocities, the ion damping decreases exponentially in the range $v_{\text{th}i} \ll v_p < c_s$, while the wave damping on the electrons begins to affect the excitation process, at $v_p \approx c_s$.

Figure 8 shows the dependence of the width L of the potential well as a function of v_p, for different T values. The almost linear increase of L can be related to the estimate given above of the typical wavelength of the potential perturbations, $\lambda \propto M^{1/2} v_p$, which also supports the insensitivity of the curves to the temperature ratio T.

B. The stopping power of a single ion

Before going into the study of a two-ion system, let us consider in detail the stopping power of a single HI when its velocity is lower than the thermal electron speed. The spatial derivative of Eq. (3.5) computed at the position of the test ion, $\mathbf{r}=0$, gives the stopping power, i.e.,

$$-\frac{dE}{dx} = Z N_D \left. \frac{\partial \phi_1^{(1)}}{\partial \xi} \right|_{\mathbf{r}=0}$$

$$= \frac{Z^2 N_D}{2\pi^2} \int_0^{k_{\max}} dk\, k^3 \int_0^1 d\mu \frac{\mu[Y(\mu v_p) + T Y(T^{1/2} M^{1/2} \mu v_p)]}{[k^2 + X(\mu v_p) + T X(T^{1/2} M^{1/2} \mu v_p)]^2 + [Y(\mu v_p) + T Y(T^{1/2} M^{1/2} \mu v_p)]^2} . \tag{3.18}$$

An upper limit on the k integration should be imposed since our dielectric description loses its validity for impact parameters b smaller than that corresponding to *close interaction* $b_{\pi/2}$, or, equivalently, for wave numbers k larger than $k=1/b_{\min}$. We observe that, strictly speaking, the electron and the ion response to the perturbation induced by the test ion cannot in general be separated in the sum of an electronic and an ionic contribution since in the denominator of Eq. (3.18) the dielectric permittivity contains the effects of both plasma populations. The problem then arises of the most correct choice of $k_{\max}$ below which the dielectric description of the plasma is valid. A specific discussion on this point is given in the Appendix. Here we just report the criterion which has been adopted to evaluate $k_{\max}$. First, we define a minimum impact parameter for the interaction between the test ion and plasma electrons, $b_{\min}^e$, and a corresponding quantity for the interaction between the test ion and the plasma ions, $b_{\min}^i$. Then, we choose $k_{\max}$ in Eq. (3.18) as the minimum between $1/b_{\min}^e$ and $1/b_{\min}^i$, for a given choice of the parameters of the physical system under consideration. In dimensionless quantities the

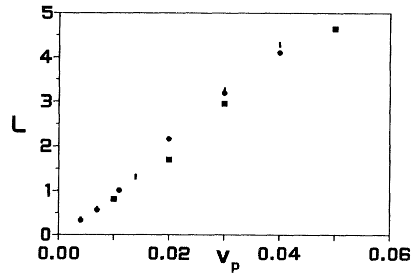

FIG. 8. The width L (in units of λ_{De}) of the first ES potential well behind the charged particle, moving in a nonisothermal plasma, as a function of the particle velocity v_p (in units of v_{the}), for the same parameters as in Fig. 7.

minimum impact parameters for each species are

$$b^e_{\min}=\frac{Z}{4\pi(v_p^2+2)}\ ,\quad b^i_{\min}=\frac{Z}{4\pi(v_p^2+2/TM)}\frac{m_e}{m_r}\ ,$$

where $m_r=m_im_p/(m_i+m_p)$ is the reduced ion mass.

Equation (3.18) has been integrated numerically for arbitrary values of the physical parameters, and approximated evaluations of the stopping power in the three velocity ranges considered in the preceding subsection have also been found analytically.

1. Stopping power for $v_p \ll v_{thi}$

Under the condition $v_p \ll (TM)^{-1/2}$, we can set approximately $Y(\xi)\approx(\pi/2)^{1/2}\xi \ll 1$, and $\mathrm{Re}\,\varepsilon \approx 1+(1+T)/k^2$. The stopping power takes the form

$$-\frac{dE}{dx}\cong\frac{Z^2N_D}{12\sqrt{2}\pi^{3/2}}v_p(1+T^{3/2}M^{1/2})\times\left[\ln\left[\frac{k^2_{\max}+T+1}{T+1}\right]-1+\frac{T+1}{k^2_{\max}+T+1}\right]. \tag{3.19}$$

2. Stopping power for $v_{thi} \ll v_p \ll c_s$

According to the considerations made in computing the corresponding ES potential, it is convenient to perform the k integration separately in the three intervals $[0,1/M^{1/2}v_p]$, $[1/M^{1/2}v_p,T^{1/2}]$, $[T^{1/2},k_{\max}]$. The first two contributions, which correspond to integration over wavelengths larger than the ion Debye length, give the *collective* part of the stopping power, while the third integral, extended over wavelength smaller than λ_{Di}, provides its *individual* part. Indeed, by considering the dominant contributions we can write

$$-\frac{dE}{dx}=-\frac{dE}{dx}\bigg|_{\rm coll}-\frac{dE}{dx}\bigg|_{\rm ind}\ , \tag{3.20}$$

where

$$-\frac{dE}{dx}\bigg|_{\rm coll}\cong\frac{Z^2N_D}{4\pi Mv_p^2}\ln(M^{1/2}T^{1/2}v_p)\ , \tag{3.20a}$$

$$-\frac{dE}{dx}\bigg|_{\rm ind}\cong\frac{Z^2N_D}{6\sqrt{2}\pi^{3/2}}v_p\ln\left[\frac{1}{\sqrt{T}}\frac{1}{b^e_{\min}}\right]+\frac{Z^2N_D}{4\pi Mv_p^2}\ln\left[\frac{1}{\sqrt{T}}\frac{1}{b^i_{\min}}\right]. \tag{3.20b}$$

It is important to observe that in computing the *individual part* of the stopping power *in the velocity range considered here,* it is possible to separate the electron and the ion response into two terms independent of each other. As a consequence it is justified to attribute to each term its own $k_{\max}$. This is *not* the case in computing the *collective part* of the stopping power.

3. Stopping power for $c_s \ll v_p \ll v_{the}$

Following the same procedure used in computing the ES potential, we get

$$-\frac{dE}{dx}\cong\frac{Z^2N_D}{8\pi Mv_p^2}\left[\ln(k^2_{\max}+1)-1+\frac{1}{k^2_{\max}+1}\right]. \tag{3.21}$$

The stopping properties of the plasma can also be conveniently described by means of the *(partial) range* defined as

$$R(E_{\rm in},E)=-\int_{E_{\rm in}}^{E}dE'\left[-\frac{dE'}{dx}\right]^{-1}. \tag{3.22}$$

It represents the length over which an ion of initial energy $E_{\rm in}$ slows down to an energy E. The complete thermalization of the projectile ion occurs over the range $R(E_{\rm in},0)$ which then represents the penetration depth.

In Fig. 9 the stopping power (in MeV/cm) is plotted as a function of the particle velocity (in cm/s) for different values of the temperature ratio T ($T_e=20$ eV and $T_i=5$, 10, 20, 40 eV). The other parameters are $Z_{\rm eff}=10$ ($Z\approx0.077$), $m_p=40$ amu, $n_0=10^{17}$ cm^{-3}. The ion and

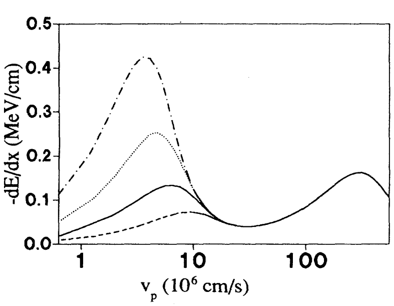

FIG. 9. The stopping power $-dE/dx$ (in MeV/cm) of a single ion, with $Z_{\rm eff}=10$ ($Z_{\rm eff}\approx0.077$) and $m_p=40$ amu, is plotted versus its velocity v_p (in 10^6 cm/s). The plasma parameters are $n_e=10^{17}$ cm^{-3}, $T_e=20$ eV, $T_i=5$ eV (dash-dotted line), 10 eV (dotted line), 20 eV (continuous line), and 40 eV (dashed line).

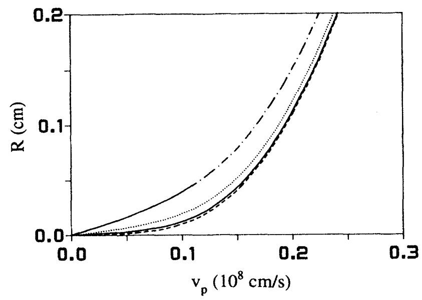

FIG. 10. The range R (in cm) of a charged particle with $m_p=40$ amu is plotted versus its velocity v_p (in 10^8 cm/s) for the same parameters as in Fig. 9.

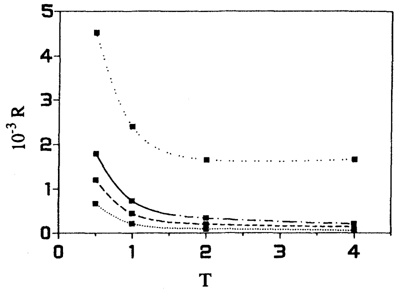

FIG. 11. The range (in units of $10^3\lambda_{De}$) of a single ion, with $Z=0.077$ and $m_p=40$ amu, is plotted versus T, for different values of its injection velocity (in units of v_{the}) $v_p=0.01$ (dotted line), 0.02 (dashed line), 0.03 (dot-dashed line), and 0.06 (double-dotted line).

the electron Bragg peaks are clearly seen. As expected, only the ion peak is affected by the T_i variation. In Fig. 10 the range $R(v_p,0)$ (in cm) is shown versus the injection velocity v_p (in cm/s), for the same parameters as in Fig. 9. Finally, in Fig. 11 the range, normalized to λ_{De}, is plotted versus T, for $m_p=40$ amu, $Z\approx 0.077$, and different values of injection velocity: $v_p=0.01,0.02,0.03,0.06$.

C. The stopping power of an ion pair

In analogy with the results of previous works on two-ion correlation effects on the stopping power of test charged particles [5,7] and of Sec. II of this paper, we expect that the presence of a second projectile at a distance of the order of or smaller than the correlation length could affect the single particle scenario considered above. We have computed the stopping power of a two-ion system moving in a plasma with the same velocity $\mathbf{v}_p$, assuming that the interparticle vector $\mathbf{d}$ remains constant in time and parallel to the velocity vector $\mathbf{v}_p$ [9,10].

The stopping power is computed by differentiating Eq. (3.3), evaluating the resulting force at the positions of the two ions, and summing up the two contributions. We get

$$-\frac{dE}{dx}=\frac{Z^2N_D}{\pi^2}\int_0^{k_{\max}}dk\,k^3\int_0^1 d\mu\frac{\mu[Y(\mu v_p)+TY(T^{1/2}M^{1/2}\mu v_p)][1+\cos(k\mu d)]}{[k^2+X(\mu v_p)+TX(T^{1/2}M^{1/2}\mu v_p)]^2+[Y(\mu v_p)+TY(T^{1/2}M^{1/2}\mu v_p)]^2}\,, \tag{3.23}$$

where Z is the dimensionless effective charge of each of the two ions assumed equal. It is seen that when the charges are very close to each other, that is, $d\to 0$, the correlation term $\cos(k\mu d)\to 1$ and the stopping power of the system becomes four times that of a single uncorrelated charge [see Eq. (3.18)], that is, twice that of a couple of uncorrelated projectiles. In the opposite limit, for $d\to\infty$, the argument of cosine oscillates very fast with k and the contribution becomes negligible. The single particle stopping power is then recovered. In the following we shall give approximated analytical expressions of Eq. (3.23) in the three velocity intervals already considered.

1. Stopping power of an ion pair for $v_p \ll v_{thi}$

At low projectile velocity, by expanding the dielectric function for small argument, we get

$$-\frac{dE}{dx}\cong\frac{Z^2N_D}{6\sqrt{2}\pi^{3/2}}v_p(1+T^{3/2}M^{1/2})\times\left[\ln\left[\frac{k_{\max}^2+T+1}{T+1}\right]-1+\frac{T+1}{k_{\max}^2+T+1}\right]. \tag{3.24}$$

It is observed that, at the dominant order in the expansions, no dependence on d appears, which means that for very slow particles two-ion correlation effects are negligible.

2. Stopping power of an ion pair for $v_{thi}\ll v_p \ll c_s$

As shown by the previous analysis of the ES potential, for $T\gg 1$ ion-acoustic oscillations are excited when the projectile velocity is in the range presently considered. Therefore we expect that correlation effects may affect the value of the stopping power. It is convenient to separate the *single particle* contribution to the stopping power from the *correlated* one:

$$-\frac{dE}{dx}=-\left.\frac{dE}{dx}\right|_{\rm sp}-\left.\frac{dE}{dx}\right|_{c}. \tag{3.25}$$

Here

$$-\left.\frac{dE}{dx}\right|_{\rm sp}\cong\frac{Z^2N_D}{2\pi M v_p^2}\ln\left[\frac{M^{1/2}v_p}{b_{\min}^i}\right]+\frac{Z^2N_D}{3\sqrt{2}\pi^{3/2}}v_p\ln\left[\frac{1}{b_{\min}^e T^{1/2}}\right] \tag{3.26}$$

and the correlated contribution has been evaluated by considering its *collective part* (long range, for $k<1$) only, i.e.,

$$-\frac{dE}{dx}\bigg|_c^{\text{coll}} \cong \frac{Z^2 N_D}{2\pi M v_p^2}\ln(T^{1/2}M^{1/2}v_p)\cos\left[\frac{d}{M^{1/2}v_p}\right]. \tag{3.27}$$

The individual particle contribution to the two-ion correlations is negligible.

In Eq. (3.27) the cosine term represents the correlation effects. Its argument, $(d/\lambda_{Di})(v_{\text{th}i}/v_p)$ in dimensional quantities, becomes smaller than unity for $d<\lambda_{\text{corr}}=\lambda_{Di}(v_p/v_{\text{th}i})$, which gives an estimate of how close the ions should be to behave in a strongly correlated way. We observe that the correlation length λ_{corr} does not depend on T_e and that the entire two-ion correlation term depends on T_e/T_i only mildly through the logarithmic term.

3. Stopping power of an ion pair for $c_s \ll v_p \ll v_{the}$

With reference to the notation of Eq. (3.25), we have approximately

$$-\frac{dE}{dx}\bigg|_{\text{sp}} \cong \frac{Z^2 N_D}{4\pi M v_p^2}\left[\ln(k_{\max}^2+1)-1+\frac{1}{k_{\max}^2+1}\right], \tag{3.28}$$

$$-\frac{dE}{dx}\bigg|_c \cong \frac{Z^2 N_D}{2\pi M v_p^2}\int_0^{k_{\max}} dk\frac{k^3}{(1+k^2)^2} \times\cos\left[\frac{kd}{\sqrt{1+k^2}M^{1/2}v_p}\right]. \tag{3.29}$$

The former contribution is just twice that of Eq. (3.21), while the latter represents the interference effects due to the vicinage of the two ions. We observe that in this velocity interval the slowing down process does not depend on T.

We present now the results of the numerical integration of Eq. (3.23). In Fig. 12 the stopping power $-dE/dx$, normalized to T_e/λ_{De}, is plotted as a function of the dimensionless ion-pair velocity v_p for different values of the dimensionless interparticle distance $d=0,0.05,0.1,0.2,0.5,1$. Dashed lines correspond to the case of uncorrelated projectiles (i.e., $d=\infty$). The parameters of the ions are $Z_{\text{eff}}=10$, $m_p=40$ amu. Two different plasmas are considered: (a) $n_e=10^{17}$ cm^{-3}, $T_e=T_i=20$ eV (corresponding to $\lambda_{De}\approx 0.1$ μm, $Z=0.086$, $N_D=116$), and (b) $n_e=10^{19}$ cm^{-3}, $T_e=100$ eV, $T_i=10$ eV ($\lambda_{De}\approx 0.02$ μm, $Z=0.077$, $N_D=137$).

In Fig. 13 the total range $R(v_p,0)$, as defined by Eq. (2.11), is plotted as a function of the injection velocity v_p of the ion pair, for different dimensionless interparticle distance, $d=0,0.05,0.2,1.5$. HI parameters are the same as those used in Fig. 12, and three sets of plasma parameters have been considered: (a) $n_e=10^{19}$ cm^{-3}, $T_e=100$ eV, $T_i=10$ eV, (b) $n_e=10^{17}$ cm^{-3}, $T_e=100$ eV, $T_i=10$ eV, and (c) $n_e=10^{17}$ cm^{-3}, $T_e=T_i=50$ eV.

In Fig. 14 the energy deposition profile of the ion pair, that is, the stopping power $-dE/dx(v)$ as a function of the corresponding partial range $R(v_p,v)$, is shown for different values of the interparticle distance: $d=0,0.05,0.2,1,5,10$. Several plasma conditions are considered: (a) $n_e=10^{19}$ cm^{-3}, $T_e=100$ eV, $T_i=10$ eV, (b) $n_e=10^{17}$ cm^{-3}, $T_e=100$ eV, $T_i=10$ eV, (c) $n_e=10^{17}$ cm^{-3}, $T_e=T_i=50$ eV, and (d) $n_e=10^{17}$ cm^{-3}, $T_e=10$ eV, $T_i=100$ eV. It is observed that by increasing T_i the ion Bragg peaks are smoothed out due to the spreading of the ion distribution function.

Finally, in Fig. 15 the range versus the dimensionless interparticle distance is plotted for $n_e=10^{17}$ cm^{-3} and three values of the temperature ratios $T=0.1,1,10$, for $Z_{\text{eff}}=10$ $m_p=40$ amu, $v_p=4\times10^7$ cm/s. Here the absolute value of $R(v_p)$ depends essentially on the electron

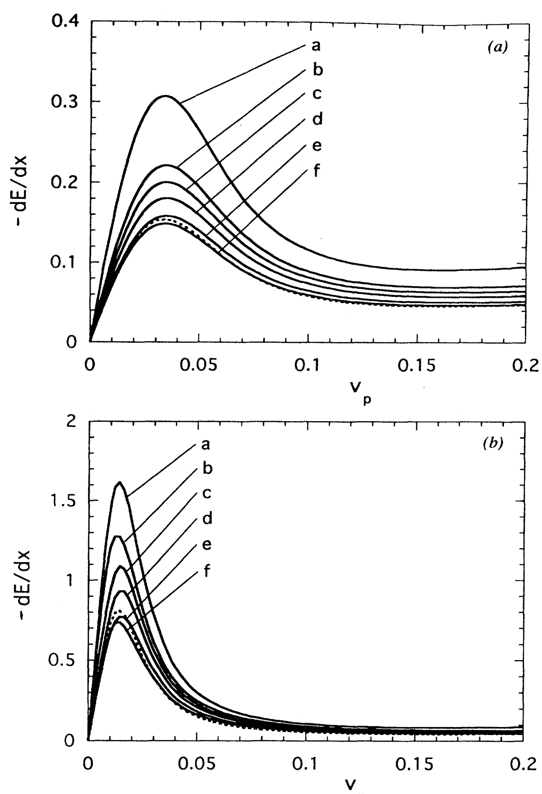

FIG. 12. The stopping power $-dE/dx$ (in units of T_e/λ_{De}) of an ion pair is plotted as a function of the projectile velocity v_p (in units of v_{the}), for different values of the interparticle distance $d=0$ (curve *a*), 0.05 (curve *b*), 0.1 (curve *c*), 0.2 (curve *d*), 0.5 (curve *e*), 1 (curve *f*). Dashed lines correspond to the case of uncorrelated particles (i.e., $d=\infty$). The parameters of the ions are $Z_{\text{eff}}=10$, $m_p=40$ amu. Two different plasmas are considered: (a) $n_e=10^{17}$ cm^{-3}, $T_e=T_i=20$ eV (corresponding to $\lambda_{De}\approx0.1$ μm, $Z=0.086$, $N_D=116$); (b) $n_e=10^{19}$ cm^{-3}, $T_e=100$ eV, $T_i=10$ eV ($\lambda_{De}\approx0.02$ μm, $Z=0.077$, $N_D=137$).

temperature, while the more extended oscillation for $T=10$ arises from the more efficient excitation of ion-acoustic waves which determine the long-range correlations. For $T=0.1$ the saturation of R versus d occurs earlier for $d \approx 1$.

IV. SUMMARY OF THE RESULTS

The present paper has dealt with the problem of the stopping power of heavy-ion pairs in a warm plasma when their motion is affected by mutual correlations. The previous analyses [4,5,7] devoted to suprathermal ($v_p \gg v_{the}$) ions have been extended to projectiles with $v_p < v_{the}$ [9,10], where the interaction with plasma ions should be retained.

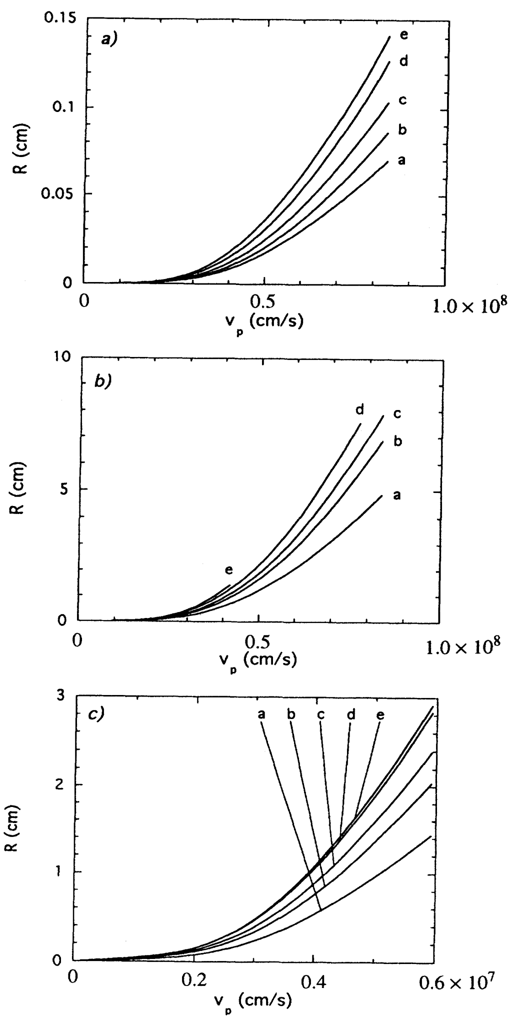

FIG. 13. The total range R (cm) of an ion pair is plotted versus the projectile velocity v_p (cm/s), for different values of the interparticle distance $d/\lambda_{De}=0$ (curve *a*), 0.05 (curve *b*), 0.2 (curve *c*), 1 (curve *d*), 5 (curve *e*). The ion parameters are the same as in Fig. 12. Three sets of plasma parameters have been considered: (a) $n_e=10^{19}$ cm^{-3}, $T_e=100$ eV, $T_i=10$ eV; (b) $n_e=10^{17}$ cm^{-3}, $T_e=100$ eV, $T_i=10$ eV; (c) $n_e=10^{17}$ cm^{-3}, $T_e=T_i=50$ eV.

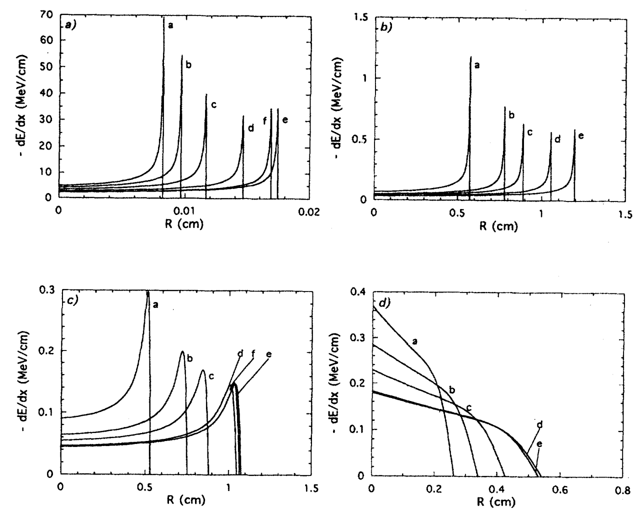

FIG. 14. The energy deposition profile of an ion pair, with $Z_{\text{eff}}=10$ and $m_p=40$ amu, i.e., $-dE/dx$ (MeV/cm) versus the partial range R (cm), is shown for different interparticle distances $d=0$ (curve *a*), 0.05 (curve *b*), 0.2 (curve *c*), 1 (curve *d*), 5 (curve *e*), 10 (curve *f*). Four different plasma conditions have been considered: (a) $n_e=10^{19}$ cm^{-3}, $T_e=100$ eV, $T_i=10$ eV; (b) $n_e=10^{17}$ cm^{-3}, $T_e=100$ eV, $T_i=10$ eV; (c) $n_e=10^{17}$ cm^{-3}, $T_e=T_i=50$ eV; (d) $n_e=10^{17}$ cm^{-3}, $T_e=10$ eV, $T_i=100$ eV.

It has been demonstrated that also at low velocities the charged projectiles generate plasma oscillations extending over several Debye lengths, depending on the particle velocity, and with amplitudes larger at higher temperature ratio(T_e/T_i) values. Conditions are then fulfilled for the occurrence of two-ion correlation if the distance between the ions of the pair is smaller than the correlation length, estimated as the wavelength of the excited oscillations.

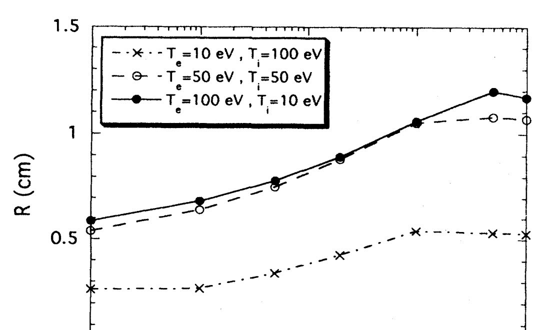

FIG. 15. The total range R (cm) of an ion pair, with $Z_{\text{eff}}=10$ and $m_p=40$ amu, is plotted versus the interparticle distance d (in units of λ_{De}) for $T_e=10$ eV and $T_i=100$ eV (dot-dashed line), $T_e=T_i=50$ eV (dashed line), $T_e=100$ eV and $T_i=10$ eV (continuous line). Other parameters are $n_e=10^{17}$ cm^{-3} and $v_p=4\times10^7$ cm/s.

A detailed study of the dependence of the ion-pair stopping power from the parameters characterizing both the projectiles and the target plasma has been carried out, showing the enhanced stopping of close ions and the consequent shortening of the range, especially in strongly nonisothermal plasmas ($T_e \gg T_i$).

The results discussed here show that the computation of the stopping power of closely spaced ions, as may occur in a dense conventional ion beam in which the ions turn out to be bunched and to reach a particularly high local density, or as it is just the case of the atoms which constitute a molecular cluster [11,12], after it has entered the target plasma, should be performed by retaining the mutual correlation effects between couples of projectiles.

The experimental observation and investigation of the correlation effects on the stopping power of relatively slow projectiles, due to their extremely reduced range ($R \cong 0.1-1$ cm) in a low atomic number high density plasma ($n_e \cong 10^{17}-10^{19}$ cm^{-3}), should be carried out by measuring the energy loss of small clusters after the interaction with a thin portion of a laser produced plasma [3,16].

Finally, it should be noted that an important consequence of an enhanced interaction between HIs and plasmas on the design of the target for an ICF based thermonuclear reactor is that it should be possible to reduce the mass of the absorber layer (in the direct drive scheme) or of the converter elements (in the indirect drive scheme), and consequently to weaken the driver energy demand to achieve the target implosion.

APPENDIX

A problem which arises when computing the energy loss of a fast charged particle in a dispersive medium by means of an average-field (dielectric) theory is the logarithmic divergence of the k integration, at large k values, or, correspondingly, of the b integration, at small impact parameters [15]. The origin of the appearance of such an unphysical divergence is usually ascribed to the lack of validity of the dielectric approach, which takes into account only weak interparticle interactions (through self-consistent fields), when one tries to include the small distance interactions, corresponding to $k \approx 1/b > 1/b_{\pi/2}$, where $b_{\pi/2}$ represents the impact parameter for a 90° deflection. With this interpretation in mind, the k integration is usually limited above by introducing the upper cutoff limit $k_{\max}=1/b_{\pi/2}$.

If the interaction of the test ion, of mass m_p and effective charge $Z_{\rm eff}$, occurs with background particles of a single charged-particle population α, we have

$$k_{\max}^{\alpha}=m_{r,\alpha}\frac{(v_p^2+2v_{\mathrm{th}\alpha}^2)}{|Z_{\rm eff}|e^2}\ , \tag{A1}$$

which depends on the species α. Here $m_{r,\alpha}=m_p m_\alpha/(m_p+m_\alpha)$ is the reduced mass in the collision between the test and the background particle.

Let us consider now a multispecies plasma (for example, composed by electrons and ions), as that for which Eq. (3.7) is to be evaluated. In this case, the argument presented above no longer leads to an unequivocal way to cut off the k integration. In fact, one can define separately two minimum impact parameters, one for the interaction with the plasma electrons and another for the interaction with the background ions.

The question is, which one of the two parameters governs the cutting off of the k integral?

This problem is closely connected to our objective of retaining the full dielectric response of the plasma. If the interaction were in a very tenuous plasma, then $\varepsilon \approx 1$, the denominator in Eq. (3.7) would be k^4, and we could separate the electron and the ion contribution to the stopping power and cutting off of each integral with its own minimum impact parameter. In this respect one could be induced to perform the same choice at high density, too, by taking

$$-\frac{dE}{dx}=\frac{Z^2N_D}{2\pi^2}\left\{\int_0^{k_{\max}^e}dk\,k^3\int_0^1 d\mu\,\mu\frac{Y_e}{[k^2+X_e+TX_i]^2+[Y_e+TY_i]^2}\right.$$
$$\left.+\int_0^{k_{\max}^i}dk\,k^3\int_0^1 d\mu\,\mu\frac{TY_i}{[k^2+X_e+TX_i]^2+[Y_e+TY_i]^2}\right\}\ , \tag{A2}$$

where $k_{\max}^e$ and $k_{\max}^i$ are defined in Eq. (A1), $X_e \equiv X(\mu v_p)$, $X_i \equiv X(T^{1/2}M^{1/2}\mu v_p)$, and similarly for Y_e and Y_i.

However, since we want to retain the complete form of the dielectric function at the denominator, even if we interpret the two addends at the numerator as representing the electron and the ion contributions, respectively, the denominator still continues to contain parts coming from either species, for which the validity of the dielectric theory should be guaranteed during the whole integration.

Then, we are led to require that the integration should be performed over all k values which guarantee the significance of the whole function which is to be integrated. As a consequence, in this paper the minimum between the $k_{\max}$ relevant to the electrons and that relevant to the ions has been chosen as an upper limit in the k integration in Eq. (3.18).

In Fig. 16 the stopping power of a single ion, with $Z_{\rm eff}=10$ and $m_p=40$ amu, computed either by using this latter choice of the cutoff parameter (continuous lines), or by separating the "electron" from the "ion" contributions to the test particle slowing down (dashed lines), has been plotted as a function of the velocity v_p. Four

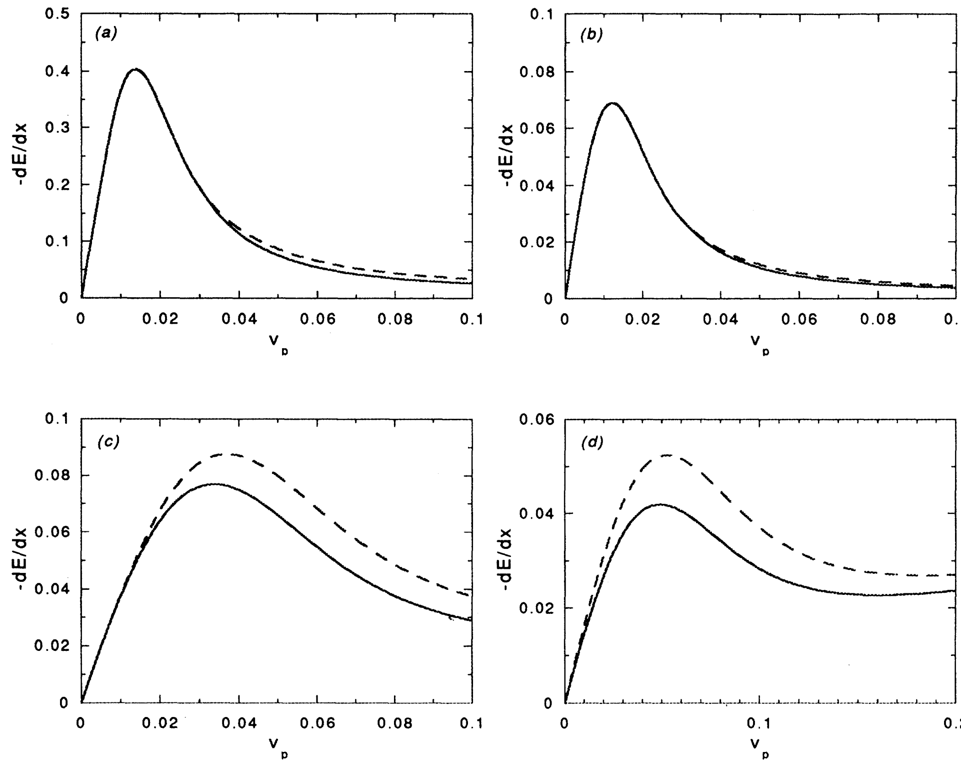

FIG. 16. The stopping power (in units of T_e/λ_{De}) of a single ion, with $Z_{\rm eff}=10$ and $m_p=40$ amu, is plotted versus its velocity v_p (in units of $v_{\rm the}$). Continuous lines refer to the choice of $k_{\rm max}$ as the minimum between the electron and the ion values, as used in the whole text. Dashed lines are obtained in the limit of tenuous plasma. Four different plasma conditions have been considered: (a) $n_e=10^{19}$ cm^{-3}, $T_e=100$ eV, $T_i=10$ eV; $n_e=10^{17}$ cm^{-3}, (b) $T_e=100$ eV, $T_i=10$ eV, (c) $T_e=T_i=20$ eV, (d) $T_e=20$ eV, $T_i=40$ eV.

different plasma conditions have been considered: (a) $n_e=10^{19}$ cm^{-3}, $T_e=100$ eV, $T_i=10$ eV; $n_e=10^{17}$ cm^{-3}, (b) $T_e=100$ eV, $T_i=10$ eV, (c) $T_e=T_i=20$ eV, (d) $T_e=20$ eV, $T_i=40$ eV.

It is observed that for $T=10$ the two procedures lead to very similar results. This is due to the fact that, for $T \gg 1$, the interaction of the test ion with the electrons and with the ions occurs in velocity ranges which are well separated. At lower values of T the collective response of the plasma to the transit of the charged projectile is such that electrons and ions participate together in the excited oscillations and in their damping, so that the stopping power computed as if the plasma were tenuous underestimates the intensity of the interaction. The only exception is for very small velocities where the friction produced by the electrons is negligible. Finally, for $T<1$ even the linear part of the stopping power, for $v_p \ll 1$, is affected by the dielectric behavior of the medium.

It is also to be noted that the differences between the two approaches seem to be more evident at higher densities, as expected. In the low density limit the two descriptions should give the same results.

[1] R. C. Arnold and J. Meyer-ter-Vehn, Rep. Prog. Phys. **50**, 559 (1987).
[2] D. H. H. Hoffmann *et al.*, Phys. Rev A **42**, 2313 (1990).
[3] C. Couillaud *et al.*, Phys. Rev. E **49**, 1545 (1994).
[4] N. R. Arista, Phys. Rev. B **18**, 1 (1978).
[5] J. D'Avanzo, M. Lontano, and P. F. Bortignon, Phys. Rev. A **45**, 6126 (1992).
[6] S. Ichimaru, *Basic Principles of Plasma Physics* (Benjamin, Reading, MA, 1973).
[7] J. D'Avanzo, M. Lontano, and P. F. Bortignon, Phys. Rev. E **47**, 3574 (1993).
[8] Th. Peter and J. Meyer-ter-Vehn, Phys. Rev. A **43**, 1998 (1991).
[9] J. D'Avanzo, E. Tome', M. Lontano, and F. Bortignon, Nuovo Cimento A **106**, 1803 (1993).
[10] E. Tome', Degree thesis, University of Milan, 1993 (unpublished).
[11] C. Deutsch, Laser Part. Beams **8**, 541 (1990).
[12] C. Deutsch and N. A. Tahir, Phys. Fluids B **4**, 3735 (1992).
[13] *Handbook of Mathematical Functions,* edited by M. Abramowitz and I. A. Stegun (Dover, New York, 1972), p. 231 ff.
[14] Th. Peter, J. Plasma. Phys. **44**, 269 (1990).
[15] W. B. Thompson and J. Hubbard, Rev. Mod. Phys. **32**, 714 (1960).
[16] C. Deutsch *et al.*, Nuovo Cimento A **106**, 1821 (1993).